UNIVERSITY OF LEEDS

This is a repository copy of *A Traveling-Wave-Based Methodology for Wide-Area Fault Location in Multiterminal DC Systems*.

White Rose Research Online URL for this paper:
http://eprints.whiterose.ac.uk/143056/

Version: Accepted Version

Article:
Azizi, S orcid.org/0000-0002-9274-1177, Sanaye-Pasand, M, Abedini, M et al. (1 more author) (2014) A Traveling-Wave-Based Methodology for Wide-Area Fault Location in Multiterminal DC Systems. IEEE Transactions on Power Delivery, 29 (6). pp. 2552-2560. ISSN 0885-8977

https://doi.org/10.1109/TPWRD.2014.2323356

© 2014 IEEE. Personal use of this material is permitted. Permission from IEEE must be obtained for all other uses, in any current or future media, including reprinting/republishing this material for advertising or promotional purposes, creating new collective works, for resale or redistribution to servers or lists, or reuse of any copyrighted component of this work in other works.

Reuse
Items deposited in White Rose Research Online are protected by copyright, with all rights reserved unless indicated otherwise. They may be downloaded and/or printed for private study, or other acts as permitted by national copyright laws. The publisher or other rights holders may allow further reproduction and re-use of the full text version. This is indicated by the licence information on the White Rose Research Online record for the item.

Takedown
If you consider content in White Rose Research Online to be in breach of UK law, please notify us by emailing eprints@whiterose.ac.uk including the URL of the record and the reason for the withdrawal request.

White Rose university consortium
Universities of Leeds, Sheffield & York

eprints@whiterose.ac.uk
https://eprints.whiterose.ac.uk/

A Traveling Wave-Based Methodology for Wide-Area Fault Location in Multi-Terminal DC Systems

Sadegh Azizi, *Student Member*, *IEEE*, Majid Sanaye-Pasand, *Senior Member*, *IEEE*,
Moein Abedini and Abbas Hassani

***Abstract*—While in many applications, multi-terminal dc (MTDC) systems are potentially appropriate substitutes for their ac counterparts, their protection problems still require more attention. This paper proposes a novel traveling wave-based methodology for fault location in MTDC systems. The traveling wave principle along with two graph theory-based lemmas is deployed to locate the fault by sectionalizing the graph representation of the MTDC system. Accordingly, the system of equations relating the fault inception time, fault point and first arrival time at different convertor locations would be derived and solved. The method merely needs the first surge arrival times, thereby eliminating the practical problems in relation with identifying subsequent traveling waves. More importantly, it successfully determines the fault location, regardless of the network topology complexity, i.e., the number of its meshes and radial lines. To demonstrate the effectiveness of the method, it is applied to some complicated MTDC systems containing both meshes and radial lines. Numerous simulation studies carried out for different conditions, verify high accuracy, robustness against fault impedance and noise immunity of the proposed method.**

***Index Terms*— Fault location, graph theory, multi-terminal dc (MTDC) system, traveling wave, wavelet transform (WT).**

NOMENCLATURE

B	Set of branches in graph G.
$D_{x,y}$	Distance between nodes x and y.
G	Graph representation of MTDC system.
i	Index of detector-equipped node.
$\boldsymbol{I}$	Set of all detector-equipped nodes.
$\boldsymbol{I}_x^{r,s}$	Set of detector indices whose first arriving surges due to a fault on segment (r,s) traverse node x.
N	Set of nodes in graph G.
$p_{x,y}^{\min}$	Shortest path between nodes x and y.
(r,s)	Segment between points r and s.
t_0	Fault inception time.
t_i^m	First surge arrival time at detector i.
$T_{x,i}$	Travel time distance between node x and detector i.
v_0	Base surge velocity.
$v_{x,y}$	Surge velocity through line (x,y).
W	Set of branch weights in graph G.
(x,y)	Branch between nodes x and y.

This work was supported by the University of Tehran under Grant 8101064-1-07.

The authors are with the School of Electrical and Computer Engineering, College of Engineering, University of Tehran, Tehran 14395-515 Iran (e-mail: sadegh.azizi@ut.ac.ir; msanaye@ut.ac.ir; m.abedini@ut.ac.ir; abbas_hasani@ut.ac.ir).

I. INTRODUCTION

HIGH voltage dc (HVDC) transmission systems are considered as strong substitutes for their ac counterparts, once the associated costs are justified. In urban areas of large cities, underground cables are preferred to overhead lines for environmental and safety concerns [1], whose high capacitance in ac operation may be troublesome. As a transmission link between wind farms and land-based grids, dc cables are preferred to submarine ac cables which cannot exchange a significant amount of active power [2]. Various aspects and potentials of multi-terminal dc (MTDC) systems, also known as dc grids for meshed dc systems, in different areas such as urban sub-transmissions, microgrids and wind farms have been addressed in [1-4]. The increasing trend for wind energy applications, along with the potentials of recently emerging voltage source converter (VSC)-based HVDCs [5], visualizes a bright prospect for the future MTDC systems.

To ensure a safe dc fault extinguishment for MTDC systems, various combinations of mechanical switches (isolators) along with dc and ac circuit breakers (CBs) may be utilized [6], [7]. Fault detection is important for these systems to separate the faulted zone. On the other hand, determination of the fault location is also required to fix the problem and restore the normal operating condition [8]. The proposed method in this paper is mainly aimed at pinpointing the exact location of fault in MTDC systems, in the offline stage.

After occurrence of a fault, the initiated voltage and current traveling waves propagate on the whole network through the conductors. Accordingly, it is possible to identity the fault location by detecting the high frequency traveling waves and analyzing their features such as magnitude, polarity and time intervals between the arriving waves [9]. The traveling wave-based techniques can be applied to both ac and dc lines, and are usually considered as a powerful method for the latter [10]. Numerous studies have shown that among various traveling wave features, it is possible to determine the fault location merely by using the arrival times at some different locations. This possibility has been realized thanks to the widely spread global positioning system (GPS) signals which can provide a

time synchronization accuracy of better than 0.1 μs [11]. Additionally, the wavelet transform (WT) as an effective tool for detecting the abrupt changes in the input signals, has been widely deployed so far [8], [9].

Two different types of traveling wave-based methods have been developed for fault location on two-terminal lines. One type uses the subsequent arrival times at one terminal [12], [13], while the other one exclusively uses the time difference between the first arriving waves at both terminals [14], [15]. Although the former, not requiring communication facilities, has been extended to teed transmission lines fault location [16], [17], it in practice undergoes some difficulties regarding detection and discrimination of reflected waves, especially for the close-in faults [14], [15]. A wide-area fault location method has been proposed in [18] utilizing a limited number of traveling wave measurements across the ac power system. Nonetheless, the method necessitates the solution of a nonlinear optimization problem. Reference [19] has presented a fault location method on large transmission networks using transient current signals measured at few line terminals.

Traveling wave-based fault location in MTDC systems is a complicated procedure due to variations of the shortest paths to different detectors versus the location of the fault point. A wavelet-based strategy for MTDC systems has been proposed in [20]. The approach requires all voltage and current measurements as well as all lines being equipped with dc CBs, which might not always be the case. Additionally, it may not be possible to provide power supply to all line terminals for measurement devices in practice. Reference [3] proposes an algorithm for locating faults on star-connected MTDC transmission lines. However, this topology is not a common MTDC system topology due to its low level of reliability [4].

This paper proposes a novel methodology for wide-area fault location in MTDC systems, using the measurements taken just at the converter stations. On the basis of two proved mathematical lemmas, the graph representation of the MTDC system is hypothetically sectionalized in a way that the shortest path from the fault point on each segment to any detector is traceable. Moreover, a low memory demanding technique is proposed to specify on which segment of the graph the fault has occurred. Then, the corresponding system of linear equations is constructed which accurately determines the fault location only using the first arrival times of traveling waves at different stations. This eliminates the practical issues for identification of other traveling wave features. The simulation results verify that the method is comprehensive and would successfully pinpoint the fault location for any MTDC topology, regardless of the number of its radial lines and meshes.

II. Traveling Wave-Based Fault Location

After occurrence of a fault on a transmission line, the originated travelling waves at the fault point start travelling toward both terminals. Fig. 1 depicts a single line connecting two terminals *x* and *y*. Assume both terminals are equipped with high sampling rate measurement units which are synchronized with the aim of GPS signals. The first surge

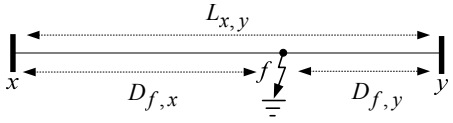

Fig. 1. Traveling wave-based fault location using two terminals measurements.

arrival time at each detector is related to a surge having traveled the shortest path from the fault point *f* to that detector. Therefore, if the first arrival times at the terminals *x* and *y* are denoted by t_x^m and t_y^m, two equations can be formed as:

$$t_x^m = t_0 + \frac{D_{f,x}}{v_{x,y}}, \tag{1}$$

$$t_y^m = t_0 + \frac{D_{f,y}}{v_{x,y}}, \tag{2}$$

where D_{fx} and D_{fy} are the lengths of the shortest paths from the fault point *f* to the terminals *x* and *y*, respectively. In addition, t_0 is the fault inception time and $v_{x,y}$ is the propagation velocity of the travelling wave. If the transmission line length is equal to $L_{x,y}$, taking into account the extra equation

$$L_{x,y} = D_{f,x} + D_{f,y}, \tag{3}$$

would result in a system of equations for three unknowns, solving of which determines the fault distance on the line and fault inception time.

The above equations would result in a precise fault location if the travelling wave arrival times at both terminals are identified. Being capable of simultaneous time and frequency domain analysis, WT has been extensively exploited for signal processing applications in power systems [8]. Since the fault location calculations are performed offline, the continuous wavelet transform (CWT) is utilized in this paper to accurately detect the abrupt changes in the measured signals [3] and [11].

It should be pointed out that the fault location problem becomes more complicated for a MTDC system including several meshes and radial lines. As opposed to a single line, the shortest path to each detector and the lines included in this path vary with respect to the fault location in the MTDC system. Hence, it is not possible to construct a unique relation such as (3) between the distances of fault point to different detectors so that it always holds true for all fault points.

III. Proposed Fault Location Methodology

In order to put forward the proposed fault location methodology, the MTDC system is represented by an undirected weighted graph. Additionally, two useful mathematical lemmas are presented. Next, the time equations corresponding to fault occurrence at different points of the MTDC system are derived. Finally, the proposed fault location algorithm is systematically presented.

A. Graph Theory Representation of MTDC Systems

Any MTDC system can be represented by a weighted graph G=(N, B, W) in which N={x,y,z,…} is the set of nodes and B={b_1,b_2,…} is the set of branches. Accordingly, the nodes and branches stand for the connection points and dc lines, respectively. Each branch b_i is identified with an unordered pair (x,y) whose elements are the end points of the respective line. Furthermore, the length of each line is considered as its corresponding branch weight and W={w_1,w_2,…} denotes the set of weights.

In a graph G, the shortest path between two nodes x and y is denoted by $P_{x,y}^{\min}$ and it can be uniquely distinguished using the set of all branches included in the path. Additionally, the distance between the two nodes x and y is defined as the sum of weights of branches included in $P_{x,y}^{\min}$ [21], which is represented by $D_{x,y}$. More generally, the shortest path can also be defined for any two points on the graph G which are not necessarily nodes. In doing so, any non-node point is considered as a new node on the G. Additionally, the branch containing the new node is divided into two new branches whose weights are proportionally assigned with respect to the location of the point on the original branch.

In order to sectionalize the graph G in a way that it is appropriate for the fault location study, the following two lemmas are proposed and proved:

Lemma I: If the shortest path between two arbitrary nodes x and y traverses a point f on the graph, this path is equivalent to the union of the shortest path between x and f, and the one between f and y.

Lemma II: Assume there is a branch between two nodes x and y, i.e., $(x, y) \in B$. If there is a shortest path between y and z traversing the node x, then for any arbitrary point f on the branch (x,y), the shortest path between f and z would traverse the node x.

Associated proofs to these lemmas are provided in Appendix.

B. Fault Equations in MTDC Systems

The first arriving wave is the one which has traveled the shortest path from the fault point to the detector. On the other hand, the velocity of surge propagation in each line (x,y), denoted by $v_{x,y}$, is known and depends on the geometry and the material of its conductors. To make the first arrival time at each detector exclusively proportional to the distance between the detector and the fault point, the weight of each branch (x,y) in the graph G is multiplied by $v_0/v_{x,y}$, where v_0 is the base surge velocity.

Suppose a line connects two points x and y, and a detector is installed at terminal z. Fig. 2 illustrates the associated graph representation. For any point f on the branch (x,y), the shortest path from f to the node z is calculated as:

$$P_{f,z}^{\min} = \min\left(P_{f,x}^{\min} \cup P_{x,z}^{\min},\ P_{f,y}^{\min} \cup P_{y,z}^{\min}\right), \tag{4}$$

or equivalently,

$$D_{f,z} = \min\left(D_{f,x} + D_{x,z}, D_{f,y} + D_{y,z}\right). \tag{5}$$

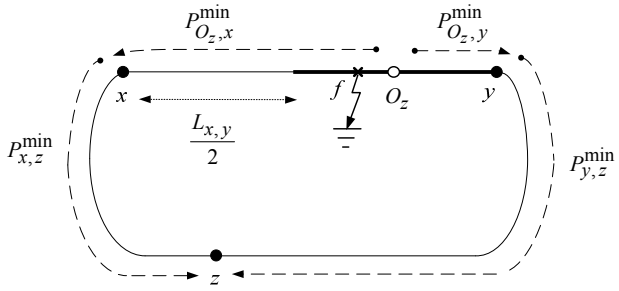

Fig. 2. Locus of symmetric point O_z, i.e., the thicker part of line (x,y).

Without loss of generality, let assume the distance between the node x and detector z is shorter than or equal to that of the node y and detector z. By taking the path between y and z which traverses the node x as an upper boundary for $P_{y,z}^{\min}$, the following constraint for $D_{y,z}$ would be derived:

$$D_{x,z} \le D_{y,z} \le D_{y,x} + D_{x,z}. \tag{6}$$

Let investigate the state in which both values in (5) are equal. Besides, let O_z be a symmetric point for which this equality constraint holds true. By equating these two values,

$$D_{O_z,x} = \frac{D_{y,z} - D_{x,z} + D_{y,x}}{2}. \tag{7}$$

From (6) and (7) together, the locus of the symmetric point O_z, whose distances from the node z in the two possible directions are equal, can be determined. Thus, for different values which may be taken by $D_{y,z}$ and $D_{x,z}$ considering the network topology, the symmetric point O_z would be certainly a point on the thicker part of the line (x,y) in Fig. 2, i.e., the 50% of the line length. Wherever the point O_z is exactly located, there exist at least two shortest paths from it to the node z, one of which traverses the node x and the other traverses the node y. According to *Lemma* II, since there is a shortest path from the point O_z to the node z traversing the node x, the shortest path from each arbitrary point f on the segment (O_z, x) to the node z would definitely contain the node x. Similarly, from all points on the segment (O_z, y), the shortest path to the node z would traverse the node y.

Now assume $\boldsymbol{I}$ is a set containing indices of all detector-equipped nodes. If on a branch (x,y), the symmetric point O_z is found for all $z \in \boldsymbol{I}$, this branch would be sectionalized into at most $|\boldsymbol{I}|$+1 segments. Here, $|\boldsymbol{I}|$ denotes the cardinality of the set $\boldsymbol{I}$, i.e., the number of its elements. Therefore, for any arbitrary point f on a so-created segment, say (r,s), it is pre-determined whether the shortest path to each detector traverses the node x or the node y. It should be noticed that this property is independent of the exact location of f on the segment (r,s). In other words, if a fault occurs on the line (x,y), it would be possible to determine that the first detected surge at each detector location has traversed which of x or y in its traveling path, if only the faulted segment is specified.

Now, the fault location methodology is discussed in two stages. First, the equations associated to a fault on any segment of the sectionalized graph of the MTDC system are derived. Then, an algorithm is proposed to determine on which segment the fault has occurred and thereby, which system of equations should be solved for the fault location.

1) Fault equations for different segments

Suppose all branches of the graph G are sectionalized with respect to the detector locations, as explained. Let (r,s) be a segment located on the branch (x,y) of the graph G. Assume $\boldsymbol{I}_x^{(r,s)}$ is a set composed of all detectors whose first detected arriving surges due to a fault at the point f on the segment (r,s) have traversed the node x in their paths. Similarly, a set $\boldsymbol{I}_y^{(r,s)}$ is defined for those whose first detected arriving surges have traversed the node y. It can be confirmed that:

$$\boldsymbol{I}_x^{(r,s)} \cup \boldsymbol{I}_y^{(r,s)} = \boldsymbol{I} \ . \tag{8}$$

Hence, if t_i^m is the first arrival time at the location i, the following two groups of time equations can be constructed:

$$t_i^m = t_0 + \frac{D_{f,x}}{v_0} + \frac{D_{x,i}}{v_0}, \qquad \forall i \in \boldsymbol{I}_x^{(r,s)} \tag{9}$$

$$t_i^m = t_0 + \frac{D_{f,y}}{v_0} + \frac{D_{y,i}}{v_0}, \qquad \forall i \in \boldsymbol{I}_y^{(r,s)}. \tag{10}$$

As the fault has occurred on the line (x,y), it can be deduced that $L_{x,y} = D_{f,x} + D_{f,y}$. By defining the topology-dependent parameters $T_{x,y} = \frac{L_{x,y}}{v_0}$, $T_{y,i} = \frac{D_{y,i}}{v_0}$ and $T_{x,i} = \frac{D_{x,i}}{v_0}$, and replacing the ratio $\frac{D_{f,x}}{v_0}$ with an unknown variable $t_{f,x}$, the following system of linear equations is obtained:

$$\begin{cases} t_i^m - T_{x,i} = t_0 + t_{f,x} & \forall i \in \boldsymbol{I}_x^{(r,s)} \\ t_i^m - T_{y,i} - T_{x,y} = t_0 - t_{f,x} & \forall i \in \boldsymbol{I}_y^{(r,s)} \end{cases} \tag{11}$$

To calculate the parameters of this system of equations, the shortest path and as a result, the distance between all node pairs, i.e., all $D_{x,y}$'s, should be found. This can be easily carried out using the effective algorithm proposed in [22].

The equations of (11) in a matrix form can be written as:

$$\boldsymbol{M} = \begin{bmatrix} \boldsymbol{H}_x^{(r,s)} \\ \boldsymbol{H}_y^{(r,s)} \end{bmatrix} \times \begin{bmatrix} t_0 \\ t_{f,x} \end{bmatrix}, \tag{12}$$

where $\boldsymbol{M}$ is a $\left(|\boldsymbol{I}_x^{(r,s)}| + |\boldsymbol{I}_y^{(r,s)}|\right) \times 1$ measurements matrix. Besides, $\boldsymbol{H}_x^{(r,s)} = \begin{bmatrix} 1 & 1 \\ \vdots & \vdots \\ 1 & 1 \end{bmatrix}_{|\boldsymbol{I}_x^{(r,s)}| \times 2}$ and $\boldsymbol{H}_y^{(r,s)} = \begin{bmatrix} 1 & -1 \\ \vdots & \vdots \\ 1 & -1 \end{bmatrix}_{|\boldsymbol{I}_y^{(r,s)}| \times 2}$.

In fact, (12) is an over-determined system of linear equations which can be solved for its two unknowns using the least-squares method. Accordingly, the fault distance and its inception time would be obtained by solving (12), given that the fault has occurred on the segment (r,s). Eventually, the fault distance on the line (x,y) in the actual MTDC system is easily calculated from $v_{x,y} \times t_{f,x}$, where $v_{x,y}$ is the surge velocity through the line (x,y).

2) Determining the faulted segment

For a fault on any segment of the sectionalized graph, a unique system of equations should be solved. On the other hand, the faulted segment is not known prior to the fault. Therefore, as a trivial approach for locating the fault, the associated system of equations (12) to each segment should be solved and its solution be found. Then, the segment would be approved as the actual faulted segment whose resulting fault distance lies between its boundaries. The basic question raised here is whether there exists an approach to distinguish the faulted segment without any need to solve all possible systems of equations. Fortunately, the answer is positive.

The system of equations (11) consists of two different groups of equations. By subtracting all possible equation pairs in each group, the following identities would be obtained:

$$\begin{cases} t_i^m - t_j^m = T_{x,i} - T_{x,j} & \forall i,j \in \boldsymbol{I}_x^{(r,s)} \\ t_i^m - t_j^m = T_{y,i} - T_{y,j} & \forall i,j \in \boldsymbol{I}_y^{(r,s)} \end{cases}. \tag{13}$$

It can be concluded that the arrival time difference between the specified detector pairs is independent of the exact fault distance on the segment (r,s). To make use of this property, the following expression is constructed between the first arrival times at different detectors, for all segments (r,s) located on a branch (x,y):

$$\sum_{\forall i,j \in \boldsymbol{I}_x^{(r,s)}} \left| (t_i^m - t_j^m) - (T_{x,i} - T_{x,j}) \right| + \sum_{\forall i,j \in \boldsymbol{I}_y^{(r,s)}} \left| (t_i^m - t_j^m) - (T_{y,i} - T_{y,j}) \right|. \tag{14}$$

According to (13), if the fault actually has occurred on this segment, (14) would be equal to zero. In practice, however, it may take a very small positive value, due to the rounding and wave front identification errors, as well as measurement devices inaccuracies.

C. Proposed Fault Location Algorithm

Based on the above explanations, an effective fault location algorithm is proposed here in two offline and online stages, as follows:

Offline stage:

I. The graph representation of the MTDC system for its current topology is derived. It should be noted that this topology is usually fixed.

II. All branches are sectionalized using (7), considering the locations of the installed detectors. Then, a set B^{new} is formed containing all segments whose terminals can be a node or a symmetric point on a branch.

III. For all segments, i.e., $\forall (r,s) \in B^{new}$ with respect to the under study branch, say (x,y), the two sets $\boldsymbol{I}_x^{(r,s)}$ and $\boldsymbol{I}_y^{(r,s)}$ are determined as explained earlier.

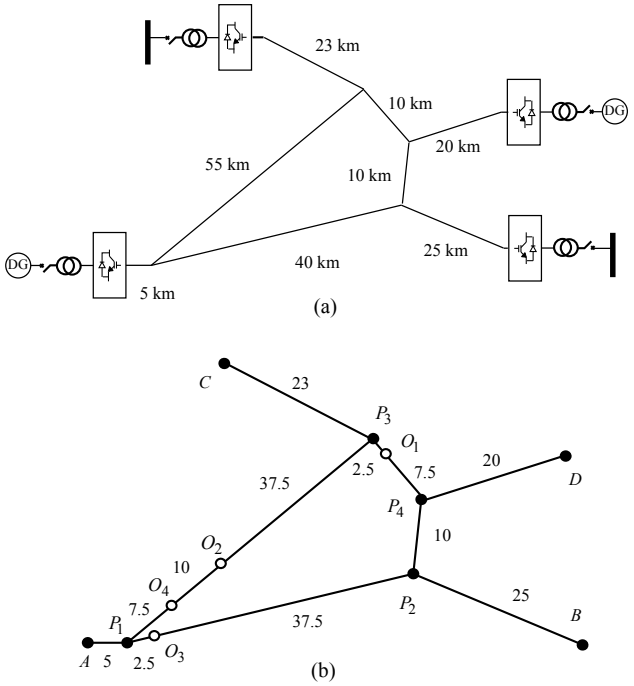

Fig. 3. (a) Monopolar MTDC system 1 with overhead lines and metallic return path. (b) Associated sectionalized graph representation.

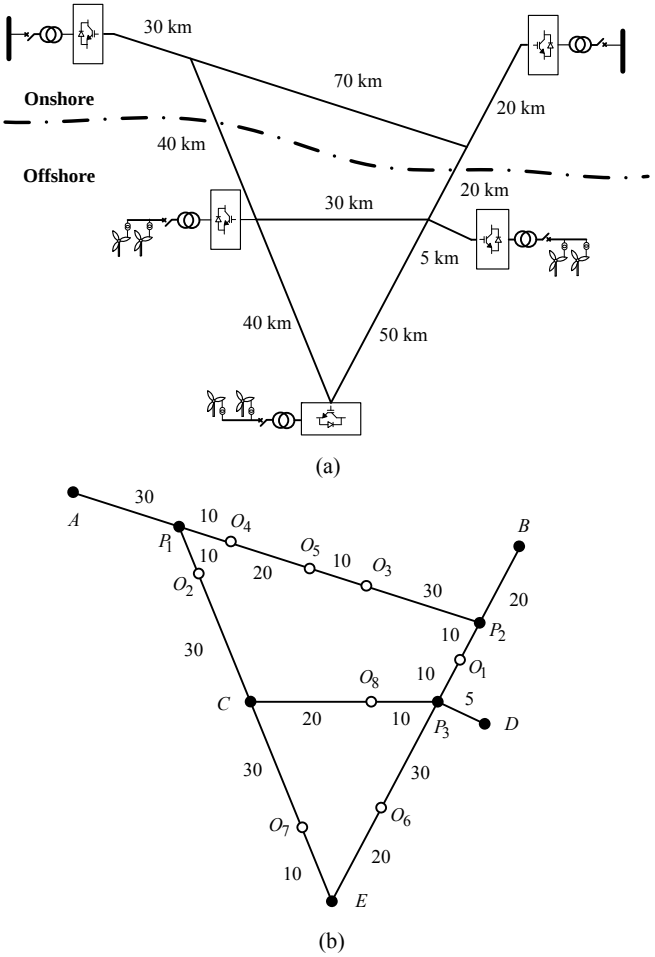

Fig. 4. (a) Monopolar MTDC system 2 with dc cables and ground return path. (b) Associated sectionalized graph representation.

Online stage:

I. The first arrival times at different detector locations across the MTDC system are derived using the WT signal processing method.

II. For all offline specified segments, i.e., $\forall(r,s) \in B^{new}$, (14) is evaluated. The segment, whose associated value is the lowest amongst all, would be considered as the faulted segment.

III. By solving the system of equations (11) for the obtained segment, the fault distance would be accurately determined.

IV. Simulation Results

To examine the efficiency of the proposed fault location method, it has been applied to a number of existing dc transmission networks and those already studied in the literature. All conducted simulations verify that the proposed method provides quite satisfactory results and it can be exploited for fault location in dc systems. Nonetheless, in order to more thoroughly investigate the potential power and usefulness of the proposed method, two complex MTDC topologies containing ring, mesh, and radial lines have been developed in this section. MTDC systems 1 and 2 are monopolar HVDC systems with metallic and ground return paths, respectively. MTDC system 1 consists of dc overhead lines. Besides, dc cable lines are exploited to construct MTDC system 2. More specifications of the studied MTDC systems are provided in Appendix.

All reported results in this section are associated with the simulation of line-to-ground faults on the proposed MTDC test systems. However, the applicability of the method has been also tested for a number of line-to-line faults in bipolar systems. As expected, the obtained results are quite accurate for the all simulated cases.

Simulations studies are carried out using PSCAD/EMTDC software [23]. Moreover, the detailed models of the HVDC converters and frequency-dependent model of the overhead lines and cables are utilized. Simulations time step is set to 0.1 μs to generate precise signals. Next, the obtained terminal current signals are sampled with a sampling frequency of 1 MHz and post-processed. The propagation velocities in the overhead and cable lines are correspondingly 297.9 and 145 m/μs which are extracted from simulation results of some known fault locations. In practice, the travelling wave propagation velocity can be obtained using the measurement of transients generated by a remote breaker switching or a fault at a known distance, or during the commissioning of the fault location system [3]. The "Haar" mother wavelet is selected for surge arrival identification. As mentioned in [3], CWT coefficients for scales in the range of 32 to 256 generally provide good results and thus scale 32 is used in this paper.

A. Fault Location Results

Two VSC-based MTDC systems, whose original and associated sectionalized graph representations are respectively shown in Figs. 3 and 4, are selected for the fault location

studies. Traveling wave detectors are installed at the converter stations. Overhead and cable dc transmission lines are correspondingly exploited to construct the first and the second MTDC systems. Meanwhile, it is important to note that the proposed method can be easily applied to any MTDC system having an arbitrary combination of overhead, cable and mixed dc lines.

It is worth noting that before a fault initiated traveling wave reaches a converter station for the first time, its control system has sensed no deviation to act in response to it. To distinguish the next arriving waves amongst many signal variations experienced afterward, the exact models of the convertor and its control system should be taken into account. Thus, it follows that the network topology and the surge propagation velocity suffice to accurately locate the fault for methods which only require the first travelling wave arrival times at detector locations [14].

In the graph representation of MTDC system 1, i.e., Fig. 3(b), 8 nodes representing the terminals and connection points are denoted by the filled circles. In addition, this graph contains 8 branches representing the dc lines. To sectionalize the graph according to the proposed method, the symmetric points considering different detector locations should be specified on various branches. Accordingly, the nodes O_1 to O_4 shown by the blank circles are obtained. Therefore, the sectionalized graph 3(b) would contain a total of 12 segments. As such, the number of segments in the sectionalized graph 4(b) is equal to 17. It should be noted that the lengths of branches are intentionally set so that the various segments have quite dissimilar lengths, in order to better reflect the capability of the proposed method.

Now, a large number of fault cases are defined and simulated for both MTDC systems. The fault impedance is altered from 0 to 200 Ω and various locations on the overhead and cable transmission lines are examined. The current measurements at detector locations are taken and post-processed using the WT to extract the associated first surge arrival times. Accordingly, numerous fault simulations are conducted whose obtained results are summarized in Table I.

TABLE I
FAULT LOCATION RESULTS

MTDC Test System	No. of Studied Fault Cases	Average Error (%)	Maximum Error (%)
1	60	0.078	0.176
2	144	0.064	0.159

TABLE II
FAULT LOCATION RESULTS FOR SOME FAULT POINTS ON LINE (P_1, P_2) OF MTDC SYSTEM 2

Fault Distance from P_1 (km)		Detector Location					Fault Inception Time (μs)	Fault Location Error (%)
		A	*B*	*C*	*D*	*E*		
		Surge Arrival Time (μs)						
10	Expected	1275.8	1551.7	1344.8	1586.2	1620.6	1000	0.032
	Detected	1279	1555	1349	1590	1624	1003.4	
35	Expected	1448.2	1379.3	1517.2	1413.7	1724.1	1000	0.056
	Detected	1453	1385	1522	1418	1727	1004.5	
50	Expected	1551.7	1275.8	1482.7	1310.3	1620.6	1000	0.062
	Detected	1556	1279	1486	1315	1625	1004.06	

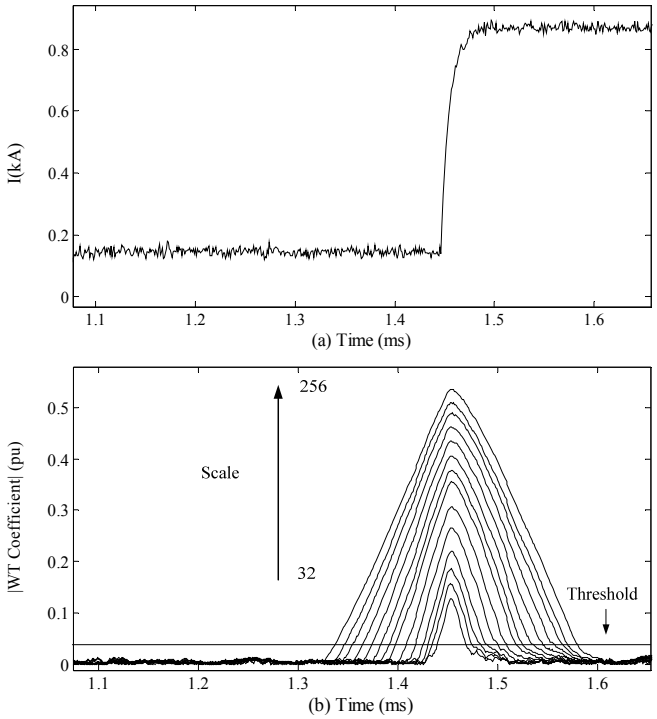

Fig. 5. (a) Contaminated current signal with 40 db white Gaussian noise. (b) WT coefficients for different scales from 32 to 256.

The absolute difference between the actual and estimated fault locations is calculated for all simulated cases. Then, the maximum and average fault location errors are obtained by dividing this difference to the respective faulted line length. As shown in Table I, the average and maximum errors are respectively 0.078% and 0.176% for MTDC system 1, and 0.064% and 0.159% for MTDC system 2. To provide more details, for three cases of faults at the beginning, middle and end of the line (P_1, P_2) in MTDC system 2, the detected surge arrival times and obtained results are listed in Table II. It can be easily confirmed that owing to a strong mathematical background, the proposed method accurately locates the fault distance and determines its inception time regardless of the complexity of the MTDC system.

B. Noise Influence on Estimation Accuracy

To investigate the influence of noise on the accuracy of the estimated fault point, the input signal is contaminated with different levels of noise. First, 40 db white Gaussian noise is added to the recorded fault current at the terminal *A*, for a fault at 35 km ahead of the point P_1 on the line (P_1, P_2) in MTDC system 2. The fault has occurred at t=1 ms and the first traveling wave arrives about 0.45 ms later. The resulting signal and associated WT coefficients are illustrated in Figs. 5(a) and 5(b), respectively. As can be seen, due to the high level of noise, the WT coefficient takes a nonzero value at the instances not corresponding to the traveling wave arrivals. Meanwhile, further simulation results reveal that for a wide range of signal to noise (SNR) ratios, the WT coefficients due to noise are not as significant as those corresponding to the traveling wave arrivals. Since noise has no meaningful information about the fault location, it would be rational to

TABLE III
NOISE INFLUENCE ON FAULT LOCATION ACCURACY

Signal to Noise Ratio (db)	Fault Distance from Point P_1 (km)				
	0	15	35	50	65
	Fault Location Error (%)				
Without Noise	0.059	0.047	0.056	0.062	0.061
70	0.059	0.047	0.056	0.062	0.061
60	0.059	0.056	0.058	0.059	0.061
50	0.064	0.056	0.058	0.073	0.061
40	0.064	0.056	0.059	0.073	0.058

define a threshold to reject the noise associated WT coefficients [15].

For a more detailed study, the SNR ratios of 70, 60, 50 and 40 db are examined, for five different fault distances on the line (P_1, P_2) of MTDC system 2. The results are tabulated in Table III. The first arrival times are properly identified by defining an appropriate threshold for detection of arriving waves at the detector locations. In addition, the added noise has no sensible influence on the first detected traveling wave arrival times. Since the magnitude of the first arriving wave is often higher than those of the subsequent ones, the methods working based on the identification of the first arriving waves provide higher noise immunity as compared to the other proposed traveling wave-based techniques.

C. Effect of Sampling Frequency

It is well-known that the fault location accuracy highly depends on the sampling rate of measurement devices. In the proposed method, the outputs of more than one measurement device are utilized for the fault location purpose. One important advantage of the suggested method is that it utilizes these values using the least-squares method. Hence, the resulting average error of the fault location would be much lower than its possible maximum. This error can be further reduced by increasing the accuracy of the measurement devices. In order to study the effect of sampling frequency on the performance of the proposed method, the sampling rate is altered from 250 kHz to 10 MHz. For five selected points on the line (P_1, P_3) in MTDC system 1, the fault location results using different sampling frequencies are given in Table IV. As expected, the estimation accuracy decreases while the sampling frequency is reduced. Besides, the noise effect is negligible. It should be pointed out that it is possible to further reduce the fault location error especially for low sampling rates using a wave front positioning correction technique suggested in [24], at the expense of some computational burden.

D. High Impedance Faults

A distinguished superiority of the proposed fault location method is its robustness against fault impedance. To verify this issue, among a number of simulated fault cases, one case is selected to be analyzed. The fault occurs at the middle of the line (C, P_3) of MTDC system 1 and the fault impedance is varied from 0 to 200 Ω. Fig. 6 shows the magnitude of the first WT coefficient peak associated to the first travelling surge arrival at detector D, in the presence of 30 db white Gaussian noise. It can be observed that as the fault impedance increases, the magnitude of the first WT coefficient peak declines. Nonetheless, the associated travelling wave arrival time remains constant, independent of the fault impedance value. Therefore, as far as the fault impedance lies within a practical range, the first arrival time at different locations is accurately identified even in the presence of noise.

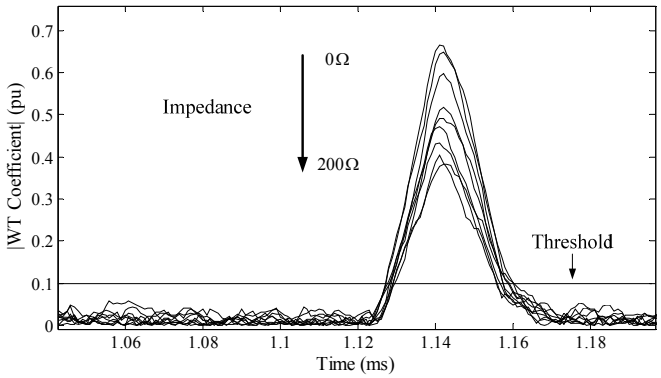

Fig. 6. Fault impedance effect on coefficient magnitude of WT applied to travelling current waves arriving at detector D.

It should be noted that treatment of bad data depends on the problem type and its formulation [25]. In this paper, the fault location problem has been formulated using the linear least-squares method to make use of all available travelling wave detectors for obtaining a result with the highest possible accuracy. As another advantage, bad data detection and identification can be easily handled in the linear least-squares context. To do so, the largest normalized residual test can be exploited to eliminate bad data and still provide an accurate fault location result [25].

V. CONCLUSION

In this paper, a novel traveling wave-based methodology was proposed for wide-area fault location in MTDC systems. The fault location algorithm is based on the traveling wave principle and is divided into two offline and online stages. In the offline stage, the graph representation of the current topology of the network is derived. Then, the obtained graph is sectionalized based on two relevant lemmas so that the shortest paths from the fault point to the various detectors are pre-specified. In the online stage, the faulted segment of the graph is determined using the identified arrival times. Next, solving the related system of equations would yield the fault

TABLE IV
EFFECT OF SAMPLING FREQUENCY ON FAULT LOCATION ACCURACY

Sampling Frequency	Fault Location Error (%)					
	Avg.	Max.	Avg.	Max.	Avg.	Max.
	Without Noise		SNR=60 db		SNR=40 db	
10 MHz	0.0135	0.0612	0.0141	0.0714	0.0139	0.0671
5 MHz	0.0421	0.1046	0.0426	0.1245	0.0433	0.1338
1MHz	0.0955	0.1568	0.0997	0.1721	0.0984	0.1883
500 kHz	0.2815	0.6262	0.3036	0.7278	0.3168	0.7169
250KHz	0.5792	1.0879	0.5843	1.1017	0.5915	1.1115

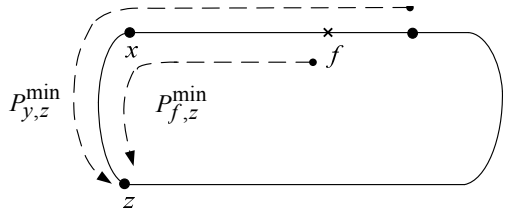

Fig. A1. Graph diagram representation of *Lemma* II.

inception time and its location.

First arrival times of the traveling waves are the only required features to be fed as inputs to the proposed fault location algorithm. Thus, the practical difficulties associated with detecting subsequent surges arrival times, extracting other features of traveling waves and their corresponding computational burdens are eliminated. It should be mentioned that the newly proposed algorithm requires just a limited number of traveling wave detectors installed at convertor stations. In addition, the proposed method can be easily applied to any MTDC system having an arbitrary combination of overhead, cable and mixed dc lines. High accuracy, noise immunity and robustness against fault impedance are among the valuable achievements of the proposed method, which have been shown in the paper. More importantly, the proposed method works properly for any MTDC system, regardless of its topology complexity, i.e., the number of its rings, meshes and radial lines.

APPENDIX

- *Lemma I*: If the shortest path between two arbitrary nodes *x* and *y* traverses a point *f* on the graph, this path is equivalent to the union of the shortest path between *x* and *f*, and the one between *f* and *y*.

Proof: The proof is quite trivial. If either of these two paths is not the shortest path, substituting it with the respective shortest one would yield a shorter path between the nodes *x* and *y* which would be a contradiction.

- *Lemma II*: Assume there is a branch between two nodes *x* and *y*, i.e., $(x, y) \in B$. If there is a shortest path between *y* and *z* traversing the node *x*, then for any arbitrary point *f* on the branch (*x*,*y*), the shortest path between *f* and *z* would traverse the node *x*.

Proof: Based on *Lemma I* and given that $P^{\min}_{y,z}$ traverses the node *x*, it can be concluded that:

$$P^{\min}_{y,z} = \{(y,x)\} \cup P^{\min}_{x,z} \Rightarrow D_{y,z} = D_{y,x} + D_{x,z} . \quad \text{(A-1)}$$

As shown in Fig. A1, the following identity holds true for the point *f* on the branch (*x*,*y*):

$$D_{y,x} = D_{y,f} + D_{f,x} . \quad \text{(A-2)}$$

Owing to being only possible to travel in two directions, all paths from the point *f* to any other node in the graph would traverse either the node *x* or the node *y*. As such, the shortest path from *f* to any node *z* is not an exception. Thus, it can be inferred from *Lemma I* that:

$$P^{\min}_{f,z} = \min\left(P^{\min}_{f,x} \cup P^{\min}_{x,z} \, , \, P^{\min}_{f,y} \cup P^{\min}_{y,z}\right). \quad \text{(A-3)}$$

According to (A-1) and (A-2), it can be easily confirmed that $D_{f,x} + D_{x,z} < D_{f,y} + D_{y,z}$. Thus, with respect to (A-3), the shortest path from the point *f* to the node *z*, i.e., $P^{\min}_{f,z}$, is the one traversing the node *x*. Hence the lemma is proved.

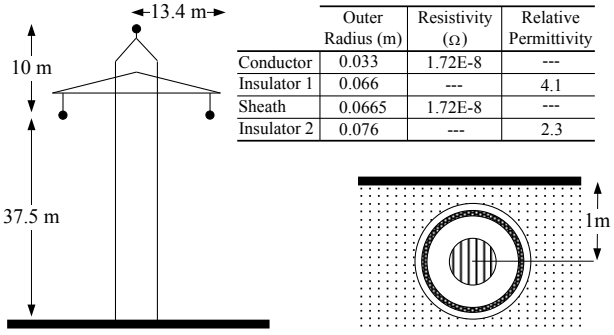

	Outer Radius (m)	Resistivity (Ω)	Relative Permittivity
Conductor	0.033	1.72E-8	---
Insulator 1	0.066	---	4.1
Sheath	0.0665	1.72E-8	---
Insulator 2	0.076	---	2.3

Fig. A2. (a) Tower structure. (b) Cable specifications.

- *Description of the Studied MTDC Systems:*

The specifications of the studied MTDC systems are provided in Table AI. Besides, the dc transmission line tower structure and the cable specifications are demonstrated in Fig. A2. For more explanation, it should be added that monopolar MTDC system 1 with nominal dc voltage of 110 kV is designed to deliver up to 55 MW of active power to each of the ac grid substations *B* and *C*. Either of two distributed generators connected through VSC to the substations *A* and *D* generates the same amount of power. Furthermore, monopolar MTDC system 2 is composed of three 300 MW wind farms at substations *C*, *D* and *E*. In addition, each of two substations *A* and *B* exports up to 450 MW to the main grid. The ac systems connected to these substations are represented by equivalent sources with the nominal frequency of 60 Hz.

TABLE AI
STUDIED MTDC SYSTEMS SPECIFICATIONS

Test System	MTDC 1	MTDC 2
System Frequency	60 Hz	60 Hz
AC Grid Voltage	132 kV	400 kV
AC Grid Short-Circuit Capacity	2000 MVA	8000 MVA
Distributed Generator Voltage	13.8 kV	33 kV
Distributed Generator Rated Power	60 MW	400 MW
DC Grid Voltage	110 kV	400 kV
AC-Side Voltage of VSC	63 kV	230 kV
Rectifier Transformer Rating	75 MVA	450 MVA
Inverter Transformer Rating	75 MVA	600 MVA
Transformer Leakage Reactance	11 %	14 %
DC Capacitor	75 μF	200 μF

REFERENCES

[1] H. Jiang and A. Ekstrom, "Multiterminal HVDC systems in urban areas of large cities," *IEEE Trans. Power Del.*, vol. 13, pp. 1278–1284, Oct. 1998.

[2] L. Weixing, B. T. Ooi, "Optimal acquisition and aggregation of offshore wind power by multiterminal voltage-source HVDC", *IEEE Trans. Power Syst.*, vol. 18, no. 1, pp. 201-206, Jan. 2003.

[3] O. M. K. K. Nanayakkara, A. D. Rajapakse, R. Wachal, "Traveling wave based line fault location in star connected multi-terminal HVDC systems," *IEEE Trans. Power Del.*, vol. 27, no. 4, pp. 2286-2294, Oct. 2012.

[4] O. Gomis-Bellmunt, J. Liang, J. Ekanayake, R. King, N. Jenkins, "Topologies of multiterminal HVDC-VSC transmission for large offshore wind farms," *Electric Power Systems Research*, vol. 81, n. 2, pp. 271-281, Feb. 2011.

[5] N. Flourentzou, V. G. Agelidis, and G. D. Demetriades, "VSC-based HVDC power transmission systems: an overview," *IEEE Trans. Power Electron*., vol 24, no 3, pp. 592-602, Mar. 2009.

[6] C. M. Franck, "HVDC circuit breakers: a review identifying future research needs", *IEEE Trans. Power Del*., vol. 26, no. 2, Apr. 2011.

[7] L. Tang, and B. Ooi, "Locating and isolating DC faults in multi-terminal DC systems", *IEEE Trans. Power Del*., vol. 22, no. 3, July 2007.

[8] Z. Galijasevic, and A. Abur, "Fault area estimation via intelligent processing of fault induced transients," *IEEE Trans. Power Syst.*, vol. 18, no. 4, pp. 1241-1247, Nov. 2003.

[9] A. Sharafi, M. Sanaye-Pasand P. Jafarian, "Ultra-high-speed protection of parallel transmission lines using current travelling waves," *IET Generation, Transmission & Distribution*., vol. 5, no. 6, pp. 656-666, Jun. 2011.

[10] Y. Zhang, N. Tai, and B. Xu, "Fault analysis and traveling-wave protection scheme for bipolar HVDC lines," *IEEE Trans. Power Del.*, vol. 27, no. 3. pp. 1583-1591, Jul. 2012.

[11] O. M. K. K. Nanayakkara, A. D. Rajapakse, and R. Wachal, "Location of dc line faults in conventional HVDC systems with segments of cables and overhead lines using terminal measurements," *IEEE Trans. Power Del.*, vol. 27, no. 1, pp. 279-288, Jan. 2012.

[12] M. Ando, E. O. Schweitzer, and R. A. Baker, "Development of field-data evaluation of single-end fault locator for two-terminal HVDC transmission," *IEEE Trans. Power Apparatus and Systems*, vol. PAS-104, no. 12, pp. 3534-3537, Dec. 1985.

[13] D. Spoor, and J. G. Zhu, "Improved single-ended traveling-wave fault location algorithm based on experience with conventional substation transducers," *IEEE Trans. Power Del*., vol. 21, no. 3, pp. 1714–1720, Jul. 2006.

[14] M. B. Dewe, S. Sankar, J. Arrillaga, "The application of satellite time references to HVDC fault location," *IEEE Trans. Power Del.,* vol. 8, no. 3, pt. 2, pp. 1295–1302, Jul. 1993.

[15] P. Jafarian and M. Sanaye-Pasand, "A traveling-wave-based protection technique using wavelet/PCA analysis," *IEEE Trans. Power Del.*, vol. 25, no. 2, pp. 588–599, Apr. 2010.

[16] S. Rajendra, and P. G. McLaren, "Travelling-wave techniques applied to the protection of teed circuits: multi-phase/multi-circuit system," *IEEE Trans. Power App. Syst.*, vol. PAS-104, no. 12, pp. 3351–3557, Dec. 1985.

[17] C. Y. Evrenosoglu, and A. Abur, "Travelling wave based fault location for teed circuits," *IEEE Trans. Power Del.*, vol. 20, no. 2, pp. 1115-1121, Apr. 2005.

[18] M. Korkali, H. Lev-Ari, and A. Abur, "Traveling-wave-based fault location technique for transmission grids via wide-area synchronized voltage measurements". *IEEE Trans. Power Syst.*, vol. 27, no. 2, pp. 1003-1011, May 2012.

[19] A. Elhaffar, N. I. Elkalashy, M. Lehtonen, "Experimental investigations on multi-end fault location system based on current traveling waves," *2007 IEEE Lausanne Power Tech*., Lausanne, Switzerland, pp. 1141-1146, Jul. 2007.

[20] K. D. Kerf, *et al.*, "Wavelet-based protection strategy for DC faults in multi-terminal VSC HVDC systems," *IET Generation, Transmission & Distribution*., vol. 5, no. 4, pp. 496-503, Sep. 2010.

[21] N. Deo, *Graph Theory with Applications to Engineering and Computer Science*. Prentice Hall: Englewood Cliffs, NJ, 1974.

[22] G. B. Dantzig, "All shortest routes in a graph," *Proceedings of the International Symposium,* Rome, Italy, pp. 91-92, Jul. 1966.

[23] PSCAD/EMTDC, Ver. 4.2 Manitoba HVDC Research Centre. 2005.

[24] X. Lin, F. Zhao, G. Wu, Z. Li, and H. Weng, "Universal wavefront positioning correction method on traveling-wave-based fault-location algorithms," *IEEE Trans. Power Del.*, vol. 27, no. 3. pp. 1601-1610, Jul. 2012.

[25] A. Abur, and A. G. Exposito, *Power System State Estimation: Theory and Implementation*, Marcel Dekker, Inc. 2004.

Sadegh Azizi (S'12) received the B.Sc. degree in electrical engineering from K. N. Toosi University of Technology in 2007 and the M.Sc. degree in electrical engineering from Sharif University of Technology, Tehran, Iran, in 2010. He is currently working toward the Ph.D. degree at the University of Tehran, Tehran, Iran.

His research interests include applications of wide-area monitoring, protection and control system in smart grids, digital protective relays and power system optimization problems.

Majid Sanaye-Pasand (M'98–SM'05) received the electrical engineering degree from the University of Tehran, Tehran, Iran, in 1988, and the M.Sc. and Ph.D. degrees from the University of Calgary, Calgary, AB, Canada, in 1994 and 1998, respectively.

Currently, he is a Professor at the School of Electrical and Computer Engineering, University of Tehran, where he is also with the Control and Intelligent Processing Center of Excellence. His areas of interest include power system analysis and control, digital protective relays, and application of artificial intelligence. He has published many papers.

Moein Abedini received the B.Sc. and M.Sc. degree in electrical engineering respectively in 2011 and 2013, from the University of Tehran, Tehran, Iran, where he is currently pursuing the Ph.D. degree.

His research interests include power system protection problems and stability studies.

Abbas Hassani received the B.Sc. degree in electrical engineering from the University of Zanjan, Zanjan, Iran. He is currently pursuing the M.Sc. degree at the University of Tehran, Tehran, Iran.

His research interests include power system studies such as applications of digital signal processing in power system analysis and power system stability.